Prediction of the Turbulent Prandtl Number in Wall Flows with Lagrangian Simulations

ARTICLE *in* INDUSTRIAL & ENGINEERING CHEMISTRY RESEARCH · NOVEMBER 2010

Impact Factor: 2.59 · DOI: 10.1021/ie1019497

2 AUTHORS, INCLUDING:

Dimitrios Papavassiliou
University of Oklahoma
174 PUBLICATIONS **1,524** CITATIONS

I&EC research
Industrial & Engineering Chemistry Research

ARTICLE

pubs.acs.org/IECR

Prediction of the Turbulent Prandtl Number in Wall Flows with Lagrangian Simulations

Chiranth Srinivasan and Dimitrios V. Papavassiliou*

School of Chemical, Biological and Materials Engineering, The University of Oklahoma, Norman, Oklahoma 73019, United States

ABSTRACT: The turbulent Prandtl number (Pr_t) is an important parameter in modeling turbulent transport, and a lot of effort has been placed in studying its behavior in wall turbulence. This work applied the Churchill model for turbulence scaling to determine the Pr_t. Two different computational approaches involving a direct numerical simulation in conjunction with Lagrangian techniques were utilized. In the first approach, the local fractions of shear stress and heat flux density, as defined using Churchill's scaling model and determined previously by Le and Papavassiliou [Le, P. M.; Papavassiliou, D. V. On temperature prediction at low Re turbulent flows using the Churchill turbulent heat flux correlation. *Int. J. Heat Mass Transfer.* **2006**, *49*, 3681−3690], were used to calculate the Pr_t. For Poiseuille channel flow, the Pr_t, at distances far away from the channel walls, was found to have a value between 0.8 and 0.9 irrespective of the molecular Prandtl number, while for plane Couette flow, it was found to be between 0.7 and 1.5. An alternative approach to determining the Pr_t is to translate Churchill's physical interpretation of Pr_t in a Lagrangian sense. Contributions of turbulent and molecular transport to momentum and heat transfer were calculated to find the local fractions of shear stress and heat flux density. For both Poiseuille channel and Couette flows, the Pr_t at $Pr = 0.1$ in regions near the center of the channel was higher than that at higher Pr. For $Pr > 0.7$, in the case of Poiseuille flow and plane Couette flow, the Pr_t started from values above 1 decreased and then followed a similar trend to that of the lower molecular Pr. The near-wall Pr_t increased with increasing Pr for both types of turbulent flow.

1. INTRODUCTION

An understanding of turbulent transfer of heat (or mass) is critical in many engineering applications, such as heat exchangers, mixers, and stirred chemical reactors. Relating the scalar fluctuations to the fluctuations in velocity is a major theoretical problem in turbulent transport. The important fundamental parameter in this case is the turbulent Prandtl number (Pr_t; or turbulent Schmidt number, Sc_t), which relates the eddy diffusivity of heat (or eddy diffusivity of mass) to the eddy diffusivity of momentum. Regarding turbulence modeling, the prediction of Pr_t is necessary to close the system of equations for heat transfer when eddy viscosity based models (such as $k-\varepsilon$ models) are utilized. Churchill,[1] in his AIChE Institute lecture, stated that, "the development of a comprehensive predictive correlative expression for the turbulent Prandtl number is the principal remaining challenge with respect to the prediction of turbulent forced convection." In analogy to its molecular counterpart, the Pr_t is defined as the ratio of eddy diffusivity of momentum to eddy diffusivity of heat, while the Sc_t is defined as the ratio of eddy diffusivity of momentum to eddy diffusivity of mass (from here on any reference to Pr_t and to heat transfer applies to the case of mass transfer and for Sc_t)

$$Pr_t = \frac{\nu_t}{\alpha_t} \tag{1}$$

The Pr_t is given as

$$Pr_t = \left(\frac{\overline{u'v'}\dfrac{\partial T}{\partial y}}{\overline{T'v'}\dfrac{\partial U}{\partial y}} \right) \tag{2}$$

The evaluation of Pr_t at any point in the turbulent flow field requires the measurement of four quantities, i.e., the turbulent Reynolds stress, the velocity gradient, the turbulent heat flux, and the temperature gradient at that point. However, the difficulty of determining these four quantities accurately and concurrently at any given point makes data available for Pr_t scarce. Most prior studies have reported that the Pr_t strongly depends on the Pr. In addition, for cases of turbulent flow through ducts, pipes, or channels, the Pr_t has shown strong dependence on the distance from the wall.

With advances in large-scale computing, several direct numerical simulation (DNS) studies of turbulent channel flows with heat transfer have been carried out.[2−8] However, only recently have DNS studies involving higher Pr been possible.[9−14] The current study is aimed at exploring the behavior of Pr_t in channel flow for different Pr's and as a function of the distance from the wall. Two turbulent flow cases that differ in the structure of the fluctuating velocity field were used, i.e., Poiseuille flow, which is driven by a pressure drop, and plane Couette flow, which is driven by the motion of the two channel walls in opposite directions. DNSs of the flow field along with the tracking of the trajectories of heat markers were utilized to calculate the turbulent shear stresses and turbulent heat flux and, in turn, to determine the Pr_t. Since the approach was the same for all Pr's,

Special Issue: Churchill Issue

Received: September 21, 2010
Accepted: November 11, 2010
Revised: November 5, 2010
Published: December 01, 2010

the study provides a consistent way of determining the Pr_t for a range of 4 orders of magnitude of Pr.

2. BACKGROUND

2.1. Turbulent Prandtl Number Modeling. Reynolds[15] provided an extensive review of prior work to determine Pr_t. Kays[16] also discussed available results for Pr_t for different fluid systems (air, water), in a two-dimensional boundary layer and in flow through a circular tube or a flat duct. The simplest model for determining Pr_t was proposed by Reynolds, who assumed that $\nu_t = \alpha_t$, resulting in a value of unity for the Pr_t. This is the well-known Reynolds analogy,[17] which is by all means an over-simplification. Several investigators have pointed out the inadequacy of the Reynolds analogy, including Churchill,[18,19] who examined the numerical and functional errors associated with using the Reynolds analogy. The widely used computational fluid dynamics software FLUENT uses a constant value of $Pr_t = 0.85$,[20] irrespective of the wall distance or the Pr. Notter and Sleicher[21] developed the following expression for Pr_t:

$$Pr_t = \frac{1 + 90Pr^{3/2}(\nu_t/\nu)^{1/4}}{[0.025Pr(\nu_t/\nu) + 90Pr^{3/2}(\nu_t/\nu)^{1/4}]\left[1 + \frac{10}{35 + (\nu_t/\nu)}\right]} \quad (3)$$

Azer and Chao[22] put forward a correlation of Pr_t for $0.6 \le Pr \le 15$ and another for the case of liquid metal fluids. The correlations predicted a dependence of Pr_t on Pr, Re, and the radial distance from the pipe wall. Jischa and Rieke[23] developed a model for Pr_t from the modeled transport equations for the turbulent kinetic energy and for the turbulent heat flux. They concluded that the dependence of the Pr_t on Re and the distance from the wall, though possible, is of second-order importance and put forth the following simple expression for Pr_t:

$$Pr_t = 0.85 + \frac{0.015}{Pr} \quad (4)$$

Among the numerous correlations proposed for Pr_t, two of the most interesting and intuitive correlations were presented by Yakhot et al.[24] and by Kays and Crawford.[25] Yakhot et al.[24] presented an analytical solution for finding Pr_t on the basis of the renormalization group method. The equation given by Yakhot et al. is

$$\left[\frac{\left(\frac{1}{Pr_{eff}} - 1.1793\right)}{\left(\frac{1}{Pr} - 1.1793\right)}\right]^{0.65}\left[\frac{\left(\frac{1}{Pr_{eff}} + 2.1793\right)}{\left(\frac{1}{Pr} + 2.1793\right)}\right]^{0.35} = \frac{1}{\left(1 + \frac{\nu_t}{\nu}\right)} \quad (5)$$

where,

$$Pr_{eff} = \frac{\left(1 + \frac{\nu_t}{\nu}\right)}{\left(\frac{\nu_t}{\nu}\frac{1}{Pr_t} + \frac{1}{Pr}\right)} \quad (6)$$

Equation 5 was suggested to be applicable for all Pr's, and at a high Pr and high values of ν_t/ν, it converges to a value of 0.85. The next important breakthrough in the prediction of Pr_t came with the empirical model of Kays and Crawford.[25] The turbulent Prandtl number according to this model is given as

$$Pr_t = \frac{1}{\left\{0.5882 + 0.228\left(\frac{\nu_t}{\nu}\right) - 0.0441\left(\frac{\nu_t}{\nu}\right)^2\left[1 - \exp\left(\frac{-5.165}{\left(\frac{\nu_t}{\nu}\right)}\right)\right]\right\}} \quad (7)$$

Both models presented above indicate that Pr_t is a function of kinematic viscosity and eddy viscosity, and it does not depend on the eddy diffusivity of heat. Kays[16] reviewed the renormalization group theory put forward by Yakhot et al.[24] and concluded that it may be applied only in the region of overlap (the logarithmic regime of the mean velocity profile). Kays proposed an expression for Pr_t that can be written as

$$Pr_t = \frac{2.0}{\left(\frac{\nu_t}{\nu}\right)Pr} + 0.85 \quad (8)$$

The coefficient 2.0 above was suggested to work better for $Pr < 1$ fluids, while a coefficient of 0.7 is appropriate for higher Pr fluids. This equation indicates that as the Pr increases, the Pr_t decreases, and for higher Pr, it approaches the value of 0.85. On the basis of the Pr_t equation developed by Kays and Crawford,[25] as shown in eq 7, Weigand et al.[26] extended the model as follows:

$$Pr_t = \frac{1}{\frac{1}{2Pr_{t\infty}} + C\,Pe_t\sqrt{\frac{1}{Pr_{t\infty}}} - (CPe_t)^2\left[1 - \exp\left(-\frac{1}{C\,Pe_t\sqrt{Pr_{t\infty}}}\right)\right]} \quad (9)$$

where,

$$Pe_t = Pr\frac{\nu_t}{\nu} \quad (10)$$

and $Pr_{t\infty}$ is the value of the Prandtl number far away from the wall, and $C = 0.3$ is a constant prescribing the spatial distribution of Pr_t vs Pe_t. Also, $Pr_{t\infty}$ was calculated by Weigand et al.[26] by the expression

$$Pr_{t\infty} = 0.85 + \frac{D}{Pr\,Re^{0.888}} \quad (11)$$

According to Weigand et al.,[26] the value of D is 100, and when eq 9 is applied, at the wall (where $Pe_t = 0$), $Pr_t \rightarrow 2Pr_{t\infty}$, while at large distances from the wall, where $Pe_t \rightarrow \infty$, it is $Pr_t \rightarrow Pr_{t\infty}$. In the original model of Kays and Crawford,[25] as shown in eq 7, $Pr_{t\infty}$ is fixed at a constant value of 0.85, which introduces an undesired behavior into the model. This model was found to do comparatively better in predicting the Pr_t for a range of Pr.

Although much work has been done to study the Pr_t for lower Pr's, very few studies have explored the effects of higher Pr on the Pr_t. Only recently have computational results with DNS or hybrid DNS−large eddy simulation become available for medium and high Pr's.[10,12] Schwertfirm and Manhart[12] have studied cases of $Pr \le 49$ and observed that in the outer region ($y^+ > 20$), the eddy conductivity is the same irrespective of the Pr. They also

observed the eddy conductivity to decrease near the wall for higher Pr's. Kasagi et al.[3,27] have used Eulerian DNS to estimate Pr_t. The recent study of Pr_t by Hasegawa and Kasagi[10] for high Pr (namely 1, 100, 200, and 400) was focused on an investigation of the asymptotic behavior of the eddy diffusivity close to the wall. It showed that there is an increase of Pr_t for increasing Pr in the viscous sublayer, but it did not present the Pr_t behavior far from the channel walls.

2.2. Turbulent Prandtl Number As a Ratio of Length Scales. Crimaldi et al.[28] proposed a model for Pr_t based on Prandtl's concept of mixing length. The turbulent Prandtl number was calculated as the ratio of the mixing length of momentum to the mixing length of heat, as follows:

$$Pr_t = \frac{L_M}{L_T} \tag{12}$$

where L_M and L_T stand for the mixing length for momentum and heat transfer, respectively. Le and Papavassiliou[29] used a Lagrangian approach in conjunction with DNS to study the correlation between the velocity and temperature fields in wall turbulence. They obtained characteristic length scales for flow structures that contribute to the transfer of heat away from the wall and characteristic length scales for momentum transfer. Assuming further that these characteristic length scales were proportional to the mixing length scales and the proportionality constant is of order 1, they used the Crimaldi et al.[28] interpretation of Pr_t, given by eq 12, to determine the Pr_t. They concluded that the Pr_t showed a dependence on the distance from the wall. However, they did not find any significant changes of the Pr_t with an increase of Pr for higher Pr's ($Pr \geq 0.7$). The estimate of the values of the Pr_t by Le and Papavassiliou was not claimed to be precise enough to distinguish effects of Pr on Pr_t.

2.3. Physical Interpretation of the Turbulent Prandtl Number Using Churchill's Turbulent Transport Model. Early work by Abbrecht and Churchill,[30] based on experiments of the flow of air in round tubes, determined the eddy viscosity and eddy diffusivity. On the basis of the ratio of these two quantities, it was concluded that Pr_t was only a function of ν_t/ν and Pr. Churchill[31,32] noted that in the case of flow through a concentric circular annulus, the locations of maximum velocity and zero in the Reynolds stress are different. This, Churchill pointed out, causes an unbounded value of eddy viscosity and mixing length, and thus, models based on these variables are not physically sound. To overcome this, Churchill and Chan[31] suggested a method to express the local time-averaged velocity and the friction factor as integrals of the turbulent shear stress, while delineating the inaccuracies that arise with convenient but physically dubious analogies.[18,19] On the basis of this line of thought, Churchill et al.[1,18,33,34] developed a theoretical framework, based on turbulence scaling other than the conventional scaling based on *viscous units* (i.e., scaling based on the friction velocity and the friction temperature) to describe turbulent scalar transport. Churchill proposed that the local fraction of shear stress due to fluctuations in velocity is a superior dimensionless variable for the modeling of turbulent flows to using dimensionless velocity obtained by scaling with the friction velocity. This local fraction of the shear stress is defined as

$$(\overline{u'v'})^{++} = -\frac{\rho \overline{u'v'}}{\tau} \tag{13}$$

The analogue of $(\overline{u'v'})^{++}$ for the transport of heat is

$$(\overline{T'v'})^{++} = \frac{\rho c \overline{T'v'}}{j} \tag{14}$$

where $(\overline{T'v'})^{++}$ is defined as the local fraction of heat flux density due to turbulence.

Using the above theory, the ratio ν_t/ν has to be equal to the ratio of the local fraction of momentum transfer due to turbulent fluctuations and to that due to molecular motions, and thus, the eddy viscosity obtained a physical meaning that is independent of its diffusive origin. Similarly, Churchill defined the eddy diffusivity over molecular diffusivity ratio to be equal to the local fraction of heat flux density due to the turbulent fluctuations and that of local heat flux density due to molecular motion. In this way, the eddy diffusivity can also be interpreted as a physical quantity that is independent of its heuristic diffusive origin. Accordingly, the mathematical expressions suggested by Churchill for the eddy viscosity and eddy diffusivity are

$$\frac{\nu_t}{\nu} = \frac{(\overline{u'v'})^{++}}{[1 - (\overline{u'v'})^{++}]} \tag{15}$$

where $[1 - (\overline{u'v'})^{++}]$ represents the local fraction of shear stress due to molecular motion, and

$$\frac{\alpha_t}{\alpha} = \frac{(\overline{T'v'})^{++}}{[1 - (\overline{T'v'})^{++}]} \tag{16}$$

where $(\overline{T'v'})^{++}$ and $[1 - (\overline{T'v'})^{++}]$ represent the local fraction of heat flux density due to turbulence and the local fraction of heat flux density due to molecular motion, respectively. Finally, the Pr_t in terms of the local fraction of fluctuations is expressed as

$$\frac{Pr_t}{Pr} = \frac{(\overline{u'v'})^{++}[1 - (\overline{T'v'})^{++}]}{(\overline{T'v'})^{++}[1 - (\overline{u'v'})^{++}]} \tag{17}$$

Within this framework, the Pr_t has an interesting and quite intuitive physical meaning. On the basis of Churchill's interpretation, the local fraction of shear stresses due to turbulence and due to molecular motion, along with the local fraction of heat flux density due to turbulence and molecular motion, are the quantities required to predict the values of Pr_t. Equation 17 suggests that Pr_t is a function of Pr, and a function of the distance from the wall, as are the local fractions of transport due to turbulence.

The above approach is free of empiricism and does not require any computational or experimental verification. The goal of the present paper, as mentioned already, is not to test the validity of the model but rather to determine the Pr_t for different Pr fluids and the behavior of the Pr_t as a function of the distance from the wall. Using DNS and a Lagrangian approach, the Pr_t was calculated using Churchill's[33] interpretation of eddy diffusivities of momentum and heat. The Pr_t was estimated with different Pr's and at different distances from the channel walls using two approaches. The first approach employed the Lagrangian scalar tracking database developed in our laboratory to generate Eulerian type mean velocity and temperature profiles. From these profiles, the variation of the local fraction of shear stress due to turbulence $(\overline{u'v'})^{++}$ and the local fraction of heat flux density due to turbulence $(\overline{T'v'})^{++}$ were determined. The details of the simulation can be found in Le and Papavassiliou.[35] The corresponding local fractions of shear stress and heat flux density due to molecular motions were also calculated, and from these values the Pr_t was calculated. The other approach involved determining the local fractions of shear stresses and normal heat flux density using the Lagrangian data directly in conjunction with Churchill's physical interpretation[33] without synthesizing any Eulerian temperature profile. This means that the Pr_t can be estimated by

finding the contributions of turbulent fluctuations to the transport of momentum and heat in the direction normal to the walls. Translating this interpretation in the Lagrangian framework, the number of fluid or heat markers that arrived at a particular distance from the wall due to turbulence would provide an estimate for the turbulence contributions to the transport of momentum or heat, while those that arrived due to molecular motion would help in calculating the molecular contributions to the transport of momentum or heat, respectively. A calculation of the ratio provided the value of Pr_t.

3. METHODOLOGY

3.1. Direct Numerical Simulation. The velocity field for channel flow was determined using the pseudospectral DNS algorithm developed by Lyons et al.[6] The simulated fluid was considered to be an incompressible Newtonian fluid with constant physical properties. The rotational form of the Navier−Stokes equation was then made dimensionless by using the kinematic viscosity, the friction velocity $u^* = (\tau_w/\rho)^{1/2}$, and the friction length and time. Periodic boundary conditions were applied in the streamwise and spanwise directions, while the no-slip, no penetration boundary conditions were applied at the channel walls. A detailed discussion of the numerical procedure and the solution of the Navier−Stokes equations were discussed in Lyons et al.[6] and validated in Gunther et al.[36] The Reynolds number, *Re*, was 2660 based on the mean centerline velocity and the channel half-height (corresponding to $Re = 10\,500$ when defined on the basis of the bulk velocity and the hydraulic diameter). The simulation was conducted on a 128 × 65 × 128 numerical mesh in the *x*, *y*, and *z* directions, respectively. The computational box was $4\pi h$, $2h$, $2\pi h$ with $h = 150$ in viscous wall units. The flow was allowed to reach the stationary state, before heat markers were released in it. The simulation time step was $\Delta t^+ = 0.125$ or 0.25 for different runs, as described in the next section depending on the approach used to determine Pr_t.

The algorithm used for the simulation of plane Couette flow was a modification of the pseudospectral DNS algorithm developed by Lyons et al.[6] The same assumptions of Newtonian and incompressible fluid with constant physical properties were applied for the plane Couette flow simulation. In Poiseuille channel flow, the mean pressure gradient was the driving force for the flow, while in the case of plane Couette flow, the driving force was constant shear stress caused by the motion of the two channel walls in opposite directions. The streamwise component of the velocity vector at the walls, which was set to zero in the case of plane Poiseuille flow, was set to ±17.739 for Couette flow. The top wall moved in the negative *x* direction, while the bottom wall moved in the positive *x* direction. The value of the wall velocity was chosen so that the *Re*, based on half the relative velocity of the two walls and the half channel height, was also 2660 for the plane Couette flow. The simulations were carried out in a 256 × 65 × 128 grid with computational box dimensions ($8\pi h$, $2h$, $2\pi h$). Prior publications[37−39] have discussed the DNS of plane Couette flow in more detail. The simulation time step was $\Delta t^+ = 0.2$ for the Couette flow case.

3.2. Lagrangian Scalar Tracking. A Lagrangian framework, where the system of reference moves along with the fluid particle, provides a more natural way to study turbulent transport. The stochastic tracking of heat or mass markers released into the flow field generated by the DNS, along with the statistical postprocessing of the results, is referred to as Lagrangian scalar tracking (LST). The calculations assume that a heat marker at each time has the same velocity as the fluid at the marker position, $\vec{V}(\vec{x}_0,t) = \vec{U}$, where $\vec{V}(\vec{x}_0,t)$ is the Lagrangian velocity of a marker that was released at a location $\vec{x}_0$ at time t_0, and $\vec{U}$ is the Eulerian velocity of the fluid at the location of the marker at time *t*. The equation of the particle motion is given as

$$\vec{V}(\vec{x}_0, t) = \frac{\partial \vec{X}(\vec{x}_0, t)}{\partial t} \tag{18}$$

The DNS, which produces the Eulerian values of velocity at each time step in a three-dimensional grid, was thus utilized to estimate the marker velocities. Since the marker positions do not coincide with the grid points, a mixed sixth-order Lagrangian−Chebyshev[40] interpolation scheme was used to estimate the fluid velocity at positions between grid points. Each marker moved due to two effects, a convective effect and a molecular diffusive effect. The convective effect was calculated by the velocities obtained at the marker positions and using an explicit, second-order Adam−Bashforth scheme. Mathematically, this time stepping algorithm can be expressed as[40]

$$X_i(x_0, t_{n+1}) = X_i(x_0, t_n) + \left[\frac{3}{2}V_i(x_0, t_n) - \frac{1}{2}V_i(x_0, t_{n-1})\right]\Delta t \tag{19}$$

The effect of molecular diffusion was estimated by imposing a three-dimensional random walk at each time step, and this was added to the convection part of the motion. The values for the random walk were taken from a Gaussian distribution with zero mean and a standard deviation of $\sigma = [(2\Delta t/Pr)]^{1/2}$, for each one of the three space dimensions in viscous wall units. The idea follows from Einstein's theory for Brownian motion. Full details of all of the Lagrangian runs used here can be found in the work of Le and Papavssiliou[37] and in Mitrovic et al.[14] Descriptions and validations for the LST methodology can be found elsewhere.[41−46]

In the first method of determining Pr_t, for Poiseuille channel flow, fluids with a *Pr* of 0.7, 3, 6, 10, and 100 were simulated, whereas for plane Couette flow, the *Pr* was 0.7, 6, 10, and 200. In both Poiseuille channel flow (these were referred to as run E, in Table 1 of ref 14) and plane Couette flow (which were referred to as run A in ref 38), 145 161 markers were released at $y_0 = 0$ at $t^+ = 0$. The time step Δt was 0.25 and 0.2 for the Poiseuille and Couette flow cases, respectively.

3.3. Incorporating Churchill's Model into the Lagrangian Framework—Local Fraction of Normal Heat Flux. Two sets of simulations were carried out to determine Pr_t for each of the Poiseuille and Couette flow cases. The first part of the simulation involved finding the local contributions of turbulence and molecular motions to normal heat flux density. The Prandtl numbers of 0.1, 0.7, 6, 10, and 100 were studied for Poiseuille channel flow, while for Couette flow Prandtl numbers of 0.1, 0.7, 3, 6, 10, and 200 were studied. In both the Poiseuille channel flow and the plane Couette flow, 145 161 heat markers were released in the flow field. The time step Δt for the simulation was 0.125 and 0.2 for the Poiseuille and Couette flow cases, respectively. The heat markers were released at $y^+ = 0$ at $t^+ = 0$ into the flow field. The channel width was divided into 300 bins, each one of width equal to one viscous unit. After the markers were uniformly dispersed in the *y* direction, which occurred at large simulation times, the markers that were within each of the 300 bins were identified and captured. Let us denote this time by t_c. Each of the heat markers captured at t_c in a bin contributed to the normal

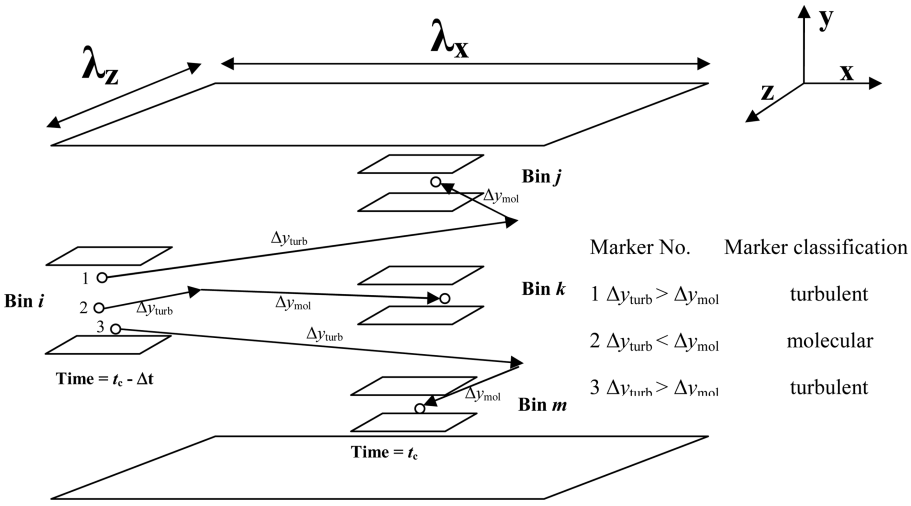

Figure 1. Schematic showing the simulation box and an example of classifying three markers that leave bin *i* and arrive at three other bins after a time interval Δt. Markers 1 and 3 in the example travel longer because of turbulence, so they would be classified as arriving at bins *j* and *m* due to turbulent motion, contributing thus to the turbulent heat flux. Marker 2, on the other hand, travels a longer distance due to molecular diffusion toward bin *k* and would be classified as arriving at bin *k* due to molecular motion (*x* is the direction of the mean flow).

heat flux in that bin; however, there needed to be a way to differentiate the ones that contributed to turbulent heat flux from those that contributed to molecular normal heat flux. The position y_{t_c} and the velocity, V_{t_c}, of all of the heat markers in each of the bins at t_c was known from the DNS/LST simulations as mentioned earlier. Note that only the vertical direction was considered, as the methodology tried to estimate the fraction of heat flux in the direction normal to the wall. As the markers moved during each time step of Δt, the position $y_{t_c+\Delta t}$ and the velocity $V_{t_c-\Delta t}$ of each heat marker were also known from the estimates of DNS/LST. The total distance a heat marker moved in that time step was estimated as $\Delta y_{tot} = y_{t_c+\Delta t} - y_{t_c}$. Using values of V_{t_c} and $V_{t_c-\Delta t}$ and substituting them in eq 19 yields the distance traveled due to convection as

$$\Delta y_{turb} = y_{t_c+\Delta t} - y_{t_c} = \left[\frac{3}{2}V_{t_c} - \frac{1}{2}V_{t_c-\Delta t}\right]\Delta t \qquad (20)$$

The distance the heat marker moved due to turbulence alone can thus be estimated. The motion of each heat marker due to molecular means can be calculated as $\Delta y_{mol} = \Delta y_{tot} - \Delta y_{turb}$. So, the values of Δy_{mol} and Δy_{turb}, for each heat marker, were compared, and depending on which was larger, a marker was labeled as a turbulent or a molecular marker. For example, if there were 2500 turbulent markers and 35 000 molecular markers found in one bin, the respective turbulent and molecular distances moved by these markers would be summed up to find the contributions of turbulent and molecular normal heat fluxes, respectively.

Figure 1 is a schematic representation of the method used to calculate the local fraction of turbulent normal heat flux for an example of three heat markers. The ratio of the turbulent to molecular normal heat fluxes, thus, provided an estimate of $(\overline{T'v'})^{++}/(1 - (\overline{T'v'})^{++})$. Now, the problem arose with the estimation of the time interval required for these calculations. This time interval was assumed to be related to the Lagrangian time scale associated with the movement of the heat markers, and more specifically it was assumed that it was proportional, i.e., a multiple, of the Lagrangian time scale. In addition, since the different regions of flow in the channel have different time scales, one common time interval for all distances from the channel wall could produce erroneous results. The Lagrangian material time scale provided a good estimate of the different time intervals that needed to be considered for different vertical locations in the channel. The expressions used were those obtained by Le and Papavassiliou:[37]

Poiseuille Flow

$$\Gamma_{Ly} = (0.98Pr^{0.13})\left[4.59 + 33.04\left(\frac{y_0}{h}\right)^{0.87}\right] \text{ for } Pr \leq 3 \qquad (21)$$

$$\Gamma_{Ly} = \left[4.59 + 33.04\left(\frac{y_0}{h}\right)^{0.87}\right] \text{ for } Pr > 3 \qquad (22)$$

Couette Flow

$$\Gamma_{Ly} = Pr^{0.083}\left[1.83 + 24.85\left(\frac{y_0}{h}\right)^{0.58}\right] \text{ for } Pr \leq 3 \qquad (23)$$

$$\Gamma_{Ly} = \left[1.83 + 24.85\left(\frac{y_0}{h}\right)^{0.58}\right] \text{ for } Pr > 3 \qquad (24)$$

As a first approach, the time intervals were calculated with substituting different values of y_0 (corresponding to locations at the center of the bins in the range 0.5−149.5) in eqs 21−24. With these values of time intervals, the local turbulent fractions of normal heat flux were determined and compared with Eulerian results for $(\overline{T'v'})^{++}$. Even though the trend observed for the local fraction of normal heat flux due to turbulence matched the results obtained from Eulerian data, there were discrepancies in the actual values. So, a calibration procedure was implemented to determine the time interval over which the movement of a heat marker should be evaluated in order to classify it as molecular or as turbulent. Two *Pr*'s, 0.7 and 10 for Poiseuille flow, were considered. The time interval was increased to twice and then to

dx.doi.org/10.1021/ie1019497 |*Ind. Eng. Chem. Res.* 2011, 50, 8881–8891

3 times Γ_{Ly} to no avail. When the time interval was fixed at 4 times Γ_{Ly}, the results matched the Eulerian results. The time interval was further increased to 5 times and then to 10 times the Lagrangian material time scale, but the resulting fraction of turbulent heat flux showed no variations. So, the time interval was determined to be four times the Lagrangian material time scale and, for all other *Pr*'s and the case of plane Couette flow, the results were also in agreement with Eulerian results. The data used to obtain the results, in the case of Poiseuille channel flow, spaned a time t_c of 2900 wall time units to 4100 wall time units, while for Couette flow, it was between 3500 and 4500 wall time units. In order to decrease noise, different initial time steps were used within these time ranges. For example, in the case of Poiseuille flow, for $Pr = 100$, at $y^+ = 149.5$, the time interval was 150 (4 times 37.5, which is the Lagrangian material time scale at $y^+ = 149.5$). In this case, 1050 different initial times starting from 2900 to 3950 were used, and the results were then averaged. Similarly, in case of Couette flow, for $Pr = 0.1$, at $y^+ = 134.5$, where the time interval was 83 (4 times 20.75), 917 different initial times were used. Also, the channel symmetry along the centerline at $y^+ = 150$ was utilized, and results for the top half of the channel were added to the results for the bottom half to further reduce statistical noise. It must be noted here that the values of Pr_t calculated were very sensitive to the values of $(\overline{T'v'})^{++}$ obtained using the above procedure, especially for the higher *Pr*'s. For example, for the case of Poiseuille flow, with $Pr = 100$, assume that the $(\overline{T'v'})^{++}$ value can be either 0.993 or 0.998, which is a difference of 0.5%. Using a value of $(\overline{u'v'})^{++}$ equal to 0.91, the Pr_t calculated utilizing eq 17 results in values of 7.128 and 2.026, respectively. This indicates that the Pr_t given by eq 17 is very sensitive to the values of $(\overline{T'v'})^{++}$, especially for higher *Pr*'s. This is an important observation, because Churchill's model for turbulent convection is insensitive to reasonable changes in the numerical and empirical functions that appear in the model equations.[47] This finding has been further corroborated with data from our laboratory,[35] but it is true for the prediction of the mean temperature profile. The prediction of Pr_t appears to be very sensitive to even very small changes in $(\overline{T'v'})^{++}$.

3.4. Incorporating Churchill's Model into the Lagrangian Framework—Local Fraction of Shear Stress. Is it possible to apply the same methodology to fluid particles (these are similar to heat markers, but their motion was simulated with no Brownian motion) and to determine the local fraction of shear stresses in the normal direction due to turbulent and molecular contributions? To resolve this question, 145 161 fluid markers were released uniformly from the $y-z$ plane at time $t^+ = 0$. The timesteps for the Poiseuille channel and plane Couette flow simulations were 0.125 and 0.2, respectively. The channel width was again separated into 300 bins of equal size, and the fluid markers that were found within each one of these bins at time t_c were identified. Similar to the estimation of the local fraction of normal heat flux, the distances traveled by turbulent and molecular fluid markers were summed up, and the ratio was used to calculate the local fraction of turbulent shear stress.

However, there were a few details that needed attention before proceeding to the calculation of the local fraction of shear stresses. First, for the motion of fluid markers, there were no diffusion effects, so the criteria to classify turbulent and molecular markers needed modification. In order to address this issue, the assumption made was that if a fluid marker left a particular bin, after moving some distance during an appropriately determined time interval, then it would be considered a turbulent marker, while if it moved from one location to another within the same bin, it would be assigned a molecular status. Hence, the number of bins (or, in other words, the bin size) is important and should be fixed.

Second, in the previous case, the Lagrangian material scale played a vital role and helped in estimating the appropriate time interval in different vertical locations of the channel. But, the same formulas cannot be applied in the case of fluid markers. This essentially left us in the dark with regards to the time interval needed. To determine the time interval, a calibration approach, as was utilized with the turbulent fraction of heat flux, was implemented. For Poiseuille channel flow, an arbitrary time interval of $\Delta t = 2$ was tried, and interestingly, the results of the local fraction of shear stress in the normal direction due to turbulence matched those from Eulerian simulations, at about $y^+ = 70.5$. So, for regions at $y^+ \geq 70.5$, the value of 2 wall time units was used to carry out the analysis and determine the local fraction of turbulent shear stress. For distances in the range $0 \leq y^+ \leq 70.5$, the use of a time interval of 2 overestimated the values; hence, the time interval needed to be smaller when compared to that at $y^+ = 70.5$. In order to determine the different time intervals, the time intervals were reduced, starting from $\Delta t = 2$ at $y^+ = 70.5$, proportional to Γ_{Ly} for Poiseuille channel flow in the vertical direction. Similarly, it was found that for plane Couette flow, a time interval of 2 matched Eulerian results at $y^+ \geq 80.5$. The different ratios of Lagrangian material scales for different y^+'s for plane Couette flow were used to determine the time intervals at distances $y^+ < 80.5$. A total of 50 and 250 different initial times for the cases of Poiseuille and plane Couette flows, respectively, were used, and the results were averaged to decrease statistical noise. The channel symmetry along $y^+ = 150$ once again was utilized to further reduce noise. The data obtained for the local fraction of turbulent shear stress for both Poiseuille and plane Couette flows agreed well with the Eulerian results reported by Le and Papavassiliou.[35]

4. RESULTS AND DISCUSSION

4.1. Turbulent Prandtl Number Obtained Using Eulerian Equations. The local fraction of shear stress due to turbulence, $(\overline{u'v'})^{++}$, can be obtained using the DNS results as follows:

$$\frac{\tau}{\tau_w}[1 - (\overline{u'v'})^{++}] = \frac{d\overline{U}^+}{dy^+} \tag{25}$$

where y^+ is the distance from the wall in viscous wall units ($y^+ = yu^*/\nu$), and $\overline{U}^+$ is the dimensionless mean velocity ($\overline{U}^+ = \overline{U}/u^*$). The value of the local fraction of shear stress due to turbulence as obtained using eq 25, for both Poiseuille[48] channel and plane Couette[35] flows, is presented in Figure 2. It starts from zero at the channel wall and goes up to nearly 1, while reaching a plateau value, at $y^+ \approx 55-60$.

The local fraction of heat flux density for the case of both walls of the channel being heated is given by[35]

$$\frac{q}{q_w}[1 - (\overline{T'v'})^{++}] = \frac{d\overline{T}^+}{dy^+} \tag{26}$$

The results obtained can be found in Figures 5a and b in ref 35.

The values of $(\overline{u'v'}^{++})$ presented in Figure 2, for Poiseuille and Couette flow, with the respective values of $(\overline{T'v'}^{++})$ (from Le and Papavassiliou[35]) are substituted into eq 17, and the Pr_t is

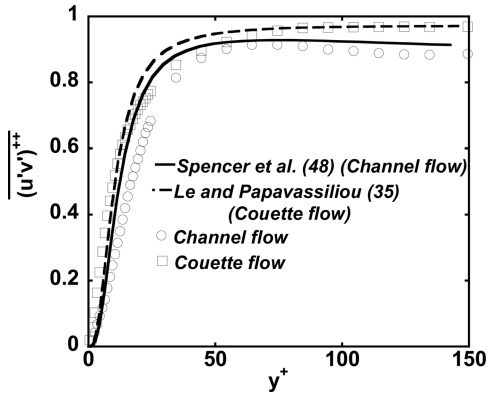

Figure 2. Local fraction of shear stress due to turbulence in the Poiseuille channel and Couette flow plotted as a function of normal distance from the wall.

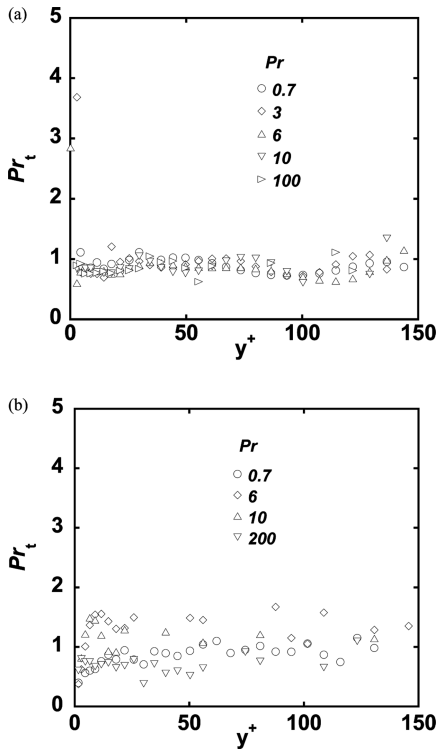

Figure 3. Turbulent Prandtl number calculated using eq 13 plotted as a function of distance from the channel wall, for the case of different molecular Prandtl numbers for (a) Poiseuille channel flow and (b) plane Couette flow.

determined as a function of the distance from the channel wall and for a range of *Pr*'s.

The results are presented in Figure 3a and b, for Poiseuille channel and plane Couette flow, respectively. For Poiseuille channel flow, the Pr_t does not show any systematic change and has values between 0.8 and 1, at large distances from channel wall, while the value increases above 1 near the channel wall. Also, the Pr_t increases with an increase in *Pr* near the channel wall. For the case of plane Couette flow, the Pr_t at large distances from the channel wall also does not exhibit systematic change, and it is between 0.7 and 1 for $Pr = 0.7$ and 200, while it is between 1 and 1.5 for $Pr = 6$ and 10. At regions close to the channel walls, the Pr_t shows lower values compared to the values at the center of the channel.

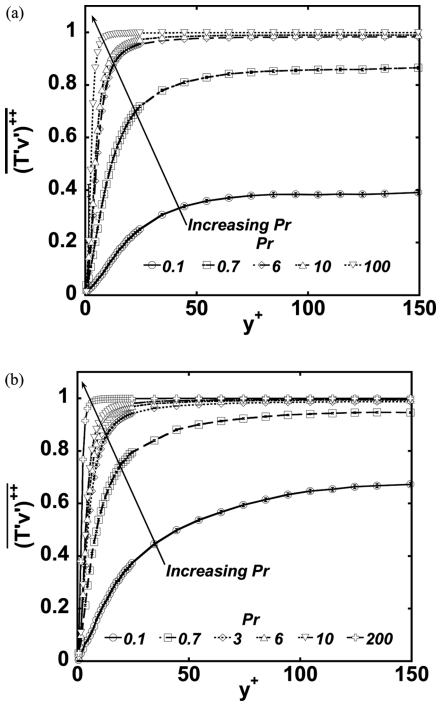

Figure 4. Local fraction of radial heat flux density due to turbulence calculated using DNS/LST and utilizing Churchill's concept plotted as a function of normal distance from the channel wall, for the case of different molecular Prandtl numbers for (a) Poiseuille channel flow and (b) plane Couette flow.

4.2. Turbulent Prandtl Number Using Lagrangian Arguments. The local fraction of turbulent shear stresses for Poiseuille and Couette flow calculated using the method described in section 3.4 is shown in Figure 2. The values obtained are a little higher than those from Eulerian calculations until $y^+ = 5.5$ and $y^+ = 13.5$, for Poiseuille flow and plane Couette flow, respectively. At distances greater than these, the values obtained for the local fraction of turbulent shear stress are always a bit lower than those from Eulerian results. However, the trend is similar for both methods, and as can be expected, the fraction of turbulent shear stress is higher near the center of the channel when compared to near the channel walls. Interestingly, for Couette flow, the fraction of turbulent shear stress is larger as compared to the Poiseuille channel flow. Such a result is in line with the fact that the turbulence intensity (i.e., the root mean squared of the velocity fluctuations) is higher for Couette flow than for Poiseuille flow at the same *Re*.

The turbulent contribution to the local fraction of normal heat flux is presented in Figure 4a and b, for Poiseuille channel and plane Couette flow, respectively, as a function of normal distance from the channel wall.

The details of the simulation methodology used to obtain these results have been discussed in section 3. The schematic shown in Figure 1 is an illustration of the idea behind the calculation of the turbulent heat flux. For both types of flow, there is zero contribution to the local fraction of normal heat flux due to turbulence at the channel walls. So, for all *Pr*'s, the curves rise from zero to values very close to one for medium-high *Pr* ($Pr \geq 3$). It is also observed that the fraction of normal heat flux due to turbulence rises faster to values close to one for higher *Pr*'s, indicating that for these *Pr*'s the normal heat flux is mainly

dx.doi.org/10.1021/ie1019497 |*Ind. Eng. Chem. Res.* 2011, 50, 8881–8891

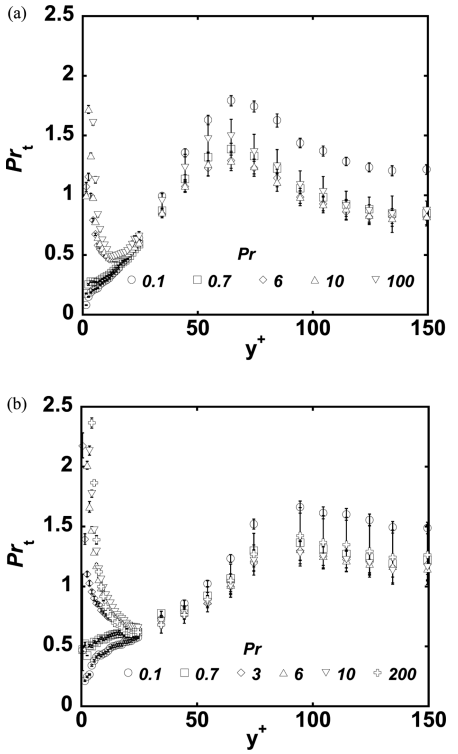

Figure 5. Turbulent Prandtl number calculated using eq 13 with data of local shear stress and radial heat flux obtained from DNS/LST and Churchill's concept plotted as a function of normal distance from the channel wall for different molecular Prandtl numbers for (a) Poiseuille channel flow and (b) plane Couette flow.

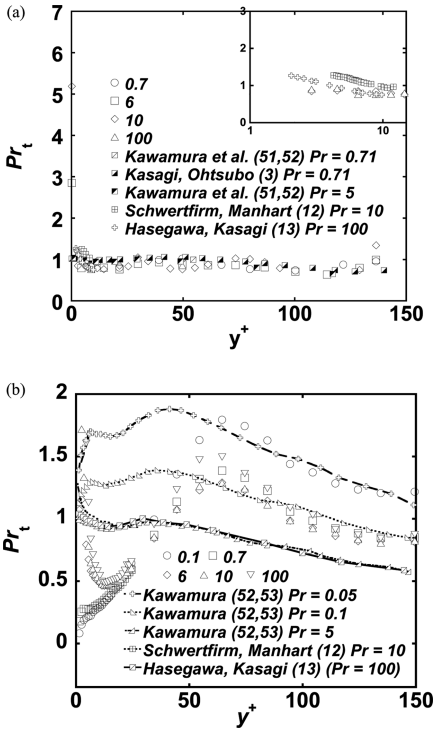

Figure 6. Turbulent Prandtl number for flow in a Poiseuille channel obtained herein compared with available data for turbulent Prandtl number and plotted as a function of normal distance from the wall for different molecular Prandtl numbers. (a) Present data obtained with eq 17. (b) Present data obtained with the process described in section 3.3.

due to turbulence. For lower *Pr*'s, this is true at large distances from the wall, while closer to the wall there are both turbulent and molecular contributions to normal heat flux. As was observed earlier for the transport of momentum, the Couette flow exhibits a higher level of turbulent contribution to the total normal heat flux than the Poiseuille channel flow. Since the Couette flow field is under constant shear stress, it can be viewed as a rather extended logarithmic layer of a turbulent velocity field. It can be, thus, inferred that the logarithmic layer is a region that promotes turbulent mixing.

Figure 5a and b are plots of the Pr_t calculated using the values of the shear stress and heat flux density from the DNS/LST. The Pr_t increases for increasing molecular *Pr* close to the wall in both Poiseuille and Couette flow. This behavior of increasing Pr_t near the wall with *Pr* has been observed previously in the DNS results of Schwertfirm and Manhart[12] and Hasegawa and Kasagi.[13] For $Pr \geq 3$, in both Poiseuille and Couette flow, the Pr_t starts from high values near the channel walls (similar to the results of Schwertfirm and Manhart[12] and Hasegawa and Kasagi[13]) and decreases as the distance from the wall increases. In the case of lower *Pr* (i.e., 0.1, 0.7), the Pr_t starts from lower values. An insight can be obtained by referring to Figure 18 of Bergant and Tiselj,[11] which showed the Pr_t profile as a function of distance from the wall, for different boundary conditions. Bergant and Tiselj[11] observed that the Pr_t showed trends of reaching a minimum near channel walls when a constant heat flux boundary condition was utilized. This boundary condition allowed temperature fluctuations at the wall. The value of Pr_t, on the other hand, increased asymptotically near channel walls, when a constant temperature boundary condition was enforced. Considering the simulation conditions of the present study, for lower *Pr*'s (i.e., $Pr = 0.1, 0.7$), the molecular diffusion effects are large compared to convective effects. So, the heat markers travel larger distances in the vertical direction, as was seen from previous results for forward dispersion (see Figure 8 of Srinivasan and Papavassiliou[49]), and the number of markers that cross the center of the bins, which can be viewed as a temperature fluctuation, is higher. For larger *Pr*'s (≥ 3), convective and diffusive effects are comparable to one another, so fewer markers move from bin to bin near the channel wall than for lower *Pr*, which translates to smaller temperature fluctuations in this case.

A comparison of the results for Pr_t using the two methods discussed here, with available data for Pr_t from earlier DNS works from Kasagi's group,[3,13,50] Kawamura et al.,[51,52] and Schwertfirm and Manhart[12] is presented in Figure 6a and b. Our results show good agreement with the previous data available for Pr_t. A comparison of the $Pr_{t\infty}$ calculated using the current method with the results from various analytical expressions discussed in section 2.1, as a function of *Pr*, is presented in Figure 7. There is qualitative agreement between the present results and these expressions. A further comparison with analytical results, not only for $Pr_{t\infty}$ but for Pr_t as a function of y^+, is shown in Figure 8. The results were obtained with a consistent methodology for *Pr* ranging from low to high values. So, this methodology using Churchill's theory provides an alternative and consistent approach to determining the Pr_t in turbulent channel flows.

dx.doi.org/10.1021/ie1019497 |*Ind. Eng. Chem. Res.* 2011, 50, 8881–8891

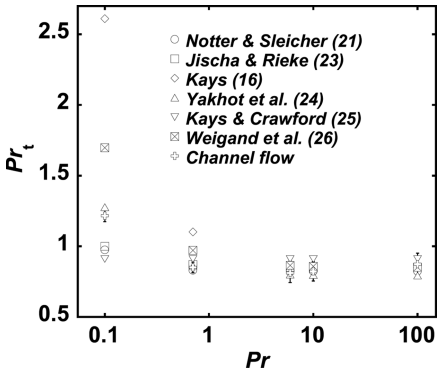

Figure 7. Value of turbulent Prandtl number far away from the wall obtained using the Lagrangian interpretation of Churchill's model (section 3.3) as a function of the molecular Prandtl number, along with results obtained by using previous correlations.

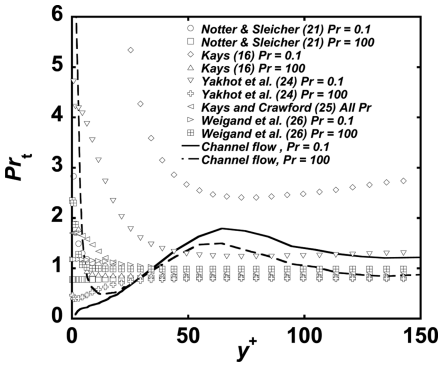

Figure 8. Turbulent Prandtl number plotted as a function of the normal distance from the wall, for a low (0.1) and high (100) molecular Prandtl number, for the present study and results obtained using correlations predicted in other previous studies.

5. CONCLUSIONS

Two methods were utilized to calculate the Pr_t. Both the methods involved Churchill's model for scaling of shear stress and heat flux in estimating the turbulent Prandtl number. The first methodology used Lagrangian data to reconstruct the Eulerian mean temperature profiles and, on the basis of the Eulerian equations of the Churchill model, yielded the local fraction of the shear stress and of the heat flux density that was attributed to turbulent effects. The second methodology involved determining the local rates of transfer utilizing a Lagrangian interpretation of Churchill's theoretical framework.

The Eulerian method gave a good estimate of the turbulent Prandtl number, and for both channel and Couette flow cases, the Pr_t was seen to be nearly constant at large distances from channel walls. The Pr_t obtained from this method did not show definitive variations with Pr. However, near channel walls, the Pr_t increased with increasing Pr, for Poiseuille channel flow, while for Couette flow, there was no observable near-wall behavior.

The Lagrangian method provided a consistent approach to modeling and calculating the Pr_t, and it provided a physical interpretation of turbulent transport. The local fraction of normal heat flux, obtained by translating Churchill's theory into scalar marker motions, was found to be in good agreement with Eulerian results. It must be emphasized that the Lagrangian material scales play a vital role in estimating the time interval that needs to be considered for the simulation at different distances from the channel walls. The fraction of turbulent normal heat flux was higher for plane Couette flow compared to Poiseuille channel flow, indicating the importance of turbulence in a constant stress region, like the logarithmic layer. The local turbulent fraction of shear stresses obtained using an analogous application of Churchill's theory also matched previous Eulerian results. For both Poiseuille and Couette flow, similar to previous results in the literature, there was an increase of Pr_t near the walls with increasing Pr. For channel flow, at large distances from channel walls, the Pr_t decreased with increasing Pr until $Pr = 6$, while for $Pr = 6$, 10, and 100, the values were very close together, considering the error bars. The same trend was observed for plane Couette flow, as for $Pr \leq 3$ there was a decrease in Pr_t with an increase in Pr, while $Pr = 6$, 10, and 200 were difficult to differentiate. This shows that Pr is important for Pr_t calculations for lower Pr's, while for higher Pr's, the differences are hardly felt. Even though the present DNS is at a relatively low Re, future advances in computer power will allow the conduction of DNS at much higher Re's. The methodology outlined in this paper would be expected to produce more accurate results as the Re increases, since Churchill's model was developed utilizing theoretical correlations and coefficients obtained from higher Re flow studies.

AUTHOR INFORMATION

Corresponding Author

*Tel.:+1-405-3255811. Fax: +1-405-3255813. E-mail: dvpapava@ou.edu.

ACKNOWLEDGMENT

On the occasion of Professor Churchill's 90th birthday, the authors would like to acknowledge his numerous contributions in the area of convective transport. His work has been the inspiration of the present study. In addition, the authors are grateful for the financial support provided by NSF under CBET-0651180. The computational support offered by the TeraGrid under TRAC TG-CTS090025 is also acknowledged. The work utilized the SGI Altix system (Cobalt) and the IBM IA-64 Linux Cluster (Mercury) at NCSA. The authors would also like to thank the OU Center for Supercomputing Education and Research (OSCER) for computer support.

NOMENCLATURE

c = heat capacity at constant pressure
C = empirical constant prescribing the spatial variation of Pr_t vs Pe_t, appearing in eq 9
k = turbulent kinetic energy
D = empirical constant appearing in eq 11
D_t = eddy diffusivity of mass
h = half channel height
j = heat flux density in the y direction
L_M = mixing length scales of momentum transfer
L_T = mixing length scales of heat transfer
Pe = Peclet number
Pe_t = turbulent Peclet number ($Pe_t = Pr\ \nu_t/\nu$)
Pr = Prandtl number ($Pr = \nu/\alpha$)
Pr_{eff} = effective Prandtl number, see eq 4
Pr_t = turbulent Prandtl number ($Pr_t = \nu_t/\alpha_t$)
$Pr_{t\infty}$ = turbulent Prandtl number far away from the wall
q = heat flux

q_w = heat flux from the wall
Sc_t = turbulent Schmidt number$(Sc_t = \nu_t/D_t)$
T = temperature
$\overline{T'v'}$ = turbulent heat flux in normal direction
$(\overline{T'v'})^{++}$ = local fraction of radial heat flux density due to turbulence
t = time
t_0, t_f = initial and final time of tracking markers
t_c = time at which the markers were captured
U = Eulerian velocity
$\overline{u'v'}$ = Reynolds stress
$(\overline{u'v'})^{++}$ = local fraction of shear stress due to turbulence
V = Lagrangian velocity in the normal direction
X, Y = Lagrangian displacement of a marker from the source in the x, y directions
x, y, z = streamwise, wall normal, and spanwise coordinates

Greek Symbols

α = thermal diffusivity
α_t = eddy diffusivity
Γ = Lagrangian material scales in the vertical direction
Δt = time step
Δy = difference in the y location
ε = rate of dissipation of turbulent energy
ν = kinematic viscosity
ν_t = eddy viscosity
π = trigonometric π (π = 3.14159...)
ρ = fluid density
σ = standard deviation of a probability density function
τ = shear stress

Superscripts and Subscripts

$\overline{(\,)}$ = ensemble average
$\vec{(\,)}$ = vector quantity
$()'$ = fluctuation
$()^+$ = value made dimensionless with the wall parameters
$()^{++}$ = local fraction due to turbulence
$()_0$ = value at the instant of marker release
$()_w$ = value at the channel wall
$()_C$ = value at the channel centerline

REFERENCES

(1) Churchill, S. W. Progress in the Thermal Sciences. *AIChE Inst. Lect., AIChE J.* **2000**, *46* (9), 1704–1722.
(2) Kim, J.; Moin, P. Transport of Passive Scalars in a Turbulent Channel Flow. *Turbulent Shear Flow* **1989**, *6*, 85–96.
(3) Kasagi, N.; Ohtsubo, Y. Direct Numerical Simulation of Low Prandtl Number Thermal Field in a Turbulent Channel Flow. *Turbulent Shear Flow* **1993**, *8*, 97–119.
(4) Kawamura, H.; Ohsaka, K.; Yamamoto, K. DNS of Turbulent Heat Transfer in Channel Flow with Low to Medium-High Prandtl Number Fluid. *Proc. 11th Symp. Turbulent Shear Flow* **1997**, *1*, 8.7–8.12.
(5) Na, Y.; Papavassiliou, D. V.; Hanratty, T. J. Use of Direct Numerical Simulation to Study the Effect of Prandtl Number on Temperature Fields. *Int. J. Heat Fluid Flow* **1999**, *20* (3), 187–195.
(6) Lyons, S. L.; Hanratty, T. J.; McLaughlin, J. B. Large-Scale Computer Simulation of Fully-Developed Turbulent Channel Flow with Heat Transfer. *Int. J. Numer. Meth. Fluids* **1991**, *13* (8), 999–028.
(7) Piller, M. Direct Numerical Simulation of Turbulent Forced Convection in a Pipe. *Int. J. Numer. Meth. Fluids* **2005**, *49*, 583–602.
(8) Redjem-Saad, L.; Ould-Rouiss, M.; Lauriat, G. Direct Numerical Simulation of Turbulent Heat Transfer in Pipe Flows: Effect of Prandtl Number. *Int. J. Heat Fluid Flow* **2007**, *28*, 847–861.
(9) Na, Y.; Hanratty, T. J. Limiting Behavior of Turbulent Scalar Transport Close to a Wall. *Int. J. Heat Mass Transfer* **2000**, *43* (10), 1749–1758.
(10) Hasegawa, Y.; Kasagi, N. Effect of Interfacial Velocity Boundary Condition on Turbulent Mass Transfer. *Int. J. Heat Fluid Flow* **2007**, *28* (6), 1192–1203.
(11) Bergant, R.; Tiselj, I. Near Wall Passive Scalar Transport at High Prandtl Numbers. *Phys. Fluids.* **2007**, *19* (6), No. 065105−1−065105−18.
(12) Schwertfirm, F.; Manhart, M. DNS of Passive Scalar Transport in Turbulent Channel Flow at High Schmidt Numbers. *Int. J. Heat Fluid Flow* **2007**, *28* (6), 1204–1214.
(13) Hasegawa, Y.; Kasagi, N. Low-Pass Filtering Effects of Viscous Sublayer on High Schmidt Number Mass Transfer Close to a Solid Wall. *Int. J. Heat Fluid Flow* **2009**, *30* (3), 525–533.
(14) Mitrovic, B. M.; Le, P. M.; Papavassiliou, D. V. On the Prandtl or Schmidt Number Dependence of the Turbulent Heat or Mass Transfer Coefficient. *Chem. Eng. Sci.* **2004**, *59* (3), 543–555.
(15) Reynolds, A. J. The Prediction of Turbulent Prandtl and Schmidt numbers. *Int. J. Heat Mass Transfer* **1975**, *18*, 1055–1069.
(16) Kays, W. M. Turbulent Prandtl Number - Where are we. *J. Heat Transfer* **1994**, *116*, 284–295.
(17) Reynolds, O. On the Extent and Action of the Heating Surface on Steam Boilers. *Proc. Lit. Philos. Soc. Manchester* **1874**, *14*, 7.*Papers on Mechanical and Physical Subjects*; Cambridge University Press: Cambridge, U. K., 1901; Vol. I, Paper 14, p 81.
(18) Churchill, S. W. New Simplified Models and Formulations for Turbulent Flow and Convection. *AIChE J.* **1997**, *43*, 1125–1140.
(19) Churchill, S. W. A Critique of the Classical Algebraic Analogies between Heat, Mass and Momentum Transfer. *Ind. Eng. Chem. Res.* **1997**, *36* (9), 3866–3878.
(20) FLUENT 6.3 User guide 12.4.5; ANSYS: Canonsburg, PA.
(21) Notter, R. D.; Sleicher, C. A. A Solution to the Turbulent Graetz Problem-III. Fully Developed and Entry Region Heat Transfer Rates. *Int. J. Heat Mass Transfer* **1972**, *27*, 2073–2093.
(22) Azer, N. T.; Chao, B. T. A mechanism of Turbulent Heat Transfer in Liquid Metals. *Int. J. Heat Mass Transfer* **1960**, *1*, 121–138.
(23) Jischa, M.; Rieke, H. B. About the Prediction of Turbulent Prandtl and Schmidt Numbers. *Int. J. Heat Mass Transfer* **1979**, *22*, 1547–1555.
(24) Yakhot, V.; Orszag, S. A.; Yakhot, A. Heat Transfer in Turbulent Fluids - 1, Pipe flow. *Int. J. Heat Mass Transfer* **1987**, *30*, 15–22.
(25) Kays, W. M.; Crawford, M. E. *Convective Heat and Mass Transfer*, 3rd ed.; McGraw-Hill: New York, 1993.
(26) Weigand, B.; Ferguson, J. R.; Crawford, M. E. An Extended Kays and Crawford Turbulent Prandtl Number Model. *Int. J. Heat Mass Transfer* **1997**, *40*, 4191–4196.
(27) Kasagi, N.; Tomita, Y.; Kurado, A. Direct Numerical Simulation of Passive Scalar Field in a Turbulent Channel Flow. *ASME J. Heat Transfer* **1992**, *114*, 598–606.
(28) Crimaldi, J. P.; Koseff, J. R.; Monismith, S. G. A Mixing Length Formulation for the Turbulent Prandtl Number in Wall-Bounded Flows with the Bed Roughness and Elevated Scalar Sources. *Phys. Fluids.* **2006**, *18* (9), No. 095102.
(29) Le, P. M.; Papavassiliou, D. V. A Physical Picture of the Mechanism of Turbulent Heat Transfer from the Wall. *Int. J. Heat Mass Transfer* **2009**, *52* (21−22), 4873–4882.
(30) Abbrecht, P. H.; Churchill, S. W. The Thermal Entrance Region in Fully Developed Turbulent Flow. *AIChE J.* **1960**, *6*, 268–273.
(31) Churchill, S. W.; Chan, C. Turbulent Flow in Channels in Terms of the Turbulent Shear and Normal Stresses. *AIChE J.* **1995**, *41*, 2513–2521.
(32) Churchill, S. W. A Critique of Predictive and Correlative Models for Turbulent Flow and Convection. *Ind. Eng. Chem. Res.* **1996**, *35*, 3122–3140.
(33) Churchill, S. W. A Reinterpretation of the Turbulent Prandtl Number. *Ind. Eng. Chem. Res.* **2002**, *41*, 6393–6401.

(34) Yu, B.; Ozoe, H.; Churchill, S. W. The Characteristics of Fully Developed Turbulent Convection in a Round Tube. *Chem. Eng. Sci.* **2001**, *56*, 1781–1800.
(35) Le, P. M.; Papavassiliou, D. V. On Temperature Prediction at Low Re Turbulent Flows using the Churchill Turbulent Heat Flux Correlation. *Int. J. Heat Mass Transfer* **2006**, *49*, 3681–3690.
(36) Gunther, A. D.; Papavassiliou, D. V.; Warholic, M. D.; Hanratty, T. J. Turbulent Flow in Channel at Low Reynolds Number. *Exp. Fluids* **1998**, *25*, 503–511.
(37) Le, P. M.; Papavassiliou, D. V. Turbulent Dispersion from Elevated Sources in Channel and Couette Flow. *AIChE J.* **2005**, *51* (9), 2402–2414.
(38) Le, P. M.; Papavassiliou, D. V. Turbulent Heat Transfer in Plane Couette Flow. *J. Heat Transfer* **2006**, *128*, 53–62.
(39) Papavassiliou, D. V.; Hanratty, T. J. Interpretation of Large-Scale Structures Observed in a Turbulent Plane Couette Flow. *Int. J. Heat Fluid Flow* **1997**, *18* (1), 55–69.
(40) Kontomaris, K.; Hanratty, T. J.; McLaughlin, J. B. An Algorithm for Tracking Fluid Particles in a Spectral Simulation of Turbulent Channel Flow. *J. Comput. Phys.* **1993**, *103*, 231–242.
(41) Papavassiliou, D. V.; Hanratty, T. J. The Use of Lagrangian Methods to Describe Transport of Heat from the Wall. *Ind. Eng. Chem. Res.* **1995**, *34*, 3359–3367.
(42) Papavassiliou, D. V.; Hanratty, T. J. Transport of a Passive Scalar in a Turbulent Channel Flow. *Int. J. Heat Mass Transfer* **1997**, *40*, 1303–1311.
(43) Ponoth, S. S.; McLaughlin, J. B. Numerical Simulation of a Mass Transfer for Bubbles in Water. *Chem. Eng. Sci.* **2000**, *55*, 1237–1255.
(44) Papavassiliou, D. V. Scalar Dispersion from an Instantaneous Line Source at the Wall of a Turbulent Channel for Medium and High Prandtl Number Fluids. *Int. J. Heat Fluid Flow* **2002**, *23*, 161–172.
(45) Papavassiliou, D. V. Turbulent Transport from Continuous Sources at the Wall of a Channel. *Int. J. Heat Mass Transfer* **2002**, *45*, 3571–3583.
(46) Mito, Y.; Hanratty, T. J. Lagrangian Stochastic Simulation of Turbulent Dispersion of Heat Markers in a Channel Flow. *Int. J. Heat Mass Transfer* **2003**, *46* (6), 1063–1073.
(47) Churchill, S. W.; Yu, B.; Kawaguchi, Y. The Accuracy and Parametric Sensitivity of Algebraic Models for Turbulent Flow and Convection. *Int. J. Heat Mass Transfer* **2005**, *48* (24−25), 5488–5503.
(48) Spencer, N. B.; Lee, L. L.; Parthasarathy, R. N.; Papavassiliou, D. V. Turbulent Structure for Poiseuille-Couette Flow and Implications for Drag Reduction over Surfaces with Slip. *Can. J. Chem. Eng.* **2009**, *87* (1), 38–46.
(49) Srinivasan, C.; Papavassiliou, D. V. Backwards and Forwards Dispersion of a Scalar in Turbulent Wall Flows. *Int. J. Heat Mass Transfer* **2010**, *53*, 1023–1035.
(50) Kasagi, N.; Ohtsubo, Y. THTLAB. http://www.thtlab.t.u-tokyo.ac.jp/ (accessed Nov 2010).
(51) Kawamura, H.; Abe, H.; Matsuo, Y. DNS of Turbulent Heat Transfer in Channel Flow with Respect to Reynolds and Prandtl Number Effects. *Int. J. Heat Fluid Flow.* **1999**, *20*, 196–207.
(52) Kawamura, H.; Ohsaka, K.; Abe, H.; Yamamoto, K. DNS of Turbulent Heat Transfer in Channel Flow with Low and Medium-High Prandtl Number Fluid. *Int. J. Heat Fluid Flow* **1998**, *19*, 482–491.